Perceptual Decision Making

Leonard Von Hollander, Sudeshna Bora

July 2020

Contents

Background

In this seminar project we would be studying the competition neural model for perceptual decision making. Perceptual decision making refers to the decision making of an individual with respect to perception. Studying the neuronal basis of perceptual decision making has found the middle temporal visual area (MT) to respond to large motion stimuli. The output of MT region further down the neural pathway activates the Lateral Intra-parietal Area (LIP) before a saccadic eye movement takes place. The LIP neuron activates if a saccadic eye movement would take place in its receptive field. Fig 1 shows the neuronal findings for LIP neurons as reported by Roitman et al [7]. Fig 1.A records the response of LIP neurons from the onset of stimuli (triangle) to initiation of saccadic motion. For saccadic motion to the receptive field of the LIP neuron population, we see an increase in firing and a decrease if the saccadic motion is away from that receptive field. The strength of firing depends upon the coherence level of the stimuli. In fig 1.B. we observe that the saccadic eye motion is initiated only when the neuron reaches a threshold. The threshold is same for different level of coherence. Also, post initiation of the stimuli, there is a dip in the firing rate. Post this dip, the discrimination regarding for or against the saccadic eye motion takes place.

This behaviour can be compared to the ramp-to-threshold

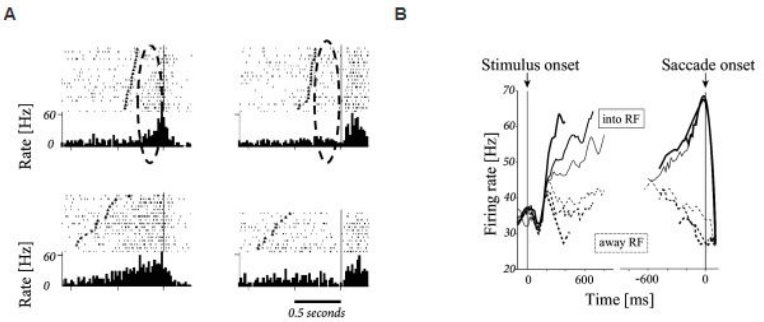

Figure 1: LIP neurons firing to motion discrimination stimuli

dynamices. The dynamics of the LIP neurons have been modeled both mathematically and bio-physiologically. Shadlen and Newsome [8] and other scientist have successfully been able to fit the neuronal behaviour to the Diffusion model. However, it leads to a long integration time in decision process, thus making it biologically implausible.

Likewise, Wang [9] was able to replicate the results of Roitman et. al[7] and Shadlen et. al [8] in his bio-physiologically based cortical microcircuit model. However, this model consists of thousands of spiking neurons that interact with each other non linearly. This makes it difficult to analyse the dynamics of the model.

This seminar project deals with a reduced version of Wang's

model as proposed by Wong et. al [10].

Model Description

Before discussing the reduced model. Let us discuss the cortical microcircuit model by Wang et. al. [9].

Cortical Micro Circuit Model

This model has been developed based on the following assumptions:-

1. Recurrent excitation of the neural network is largely mediated by NMDA receptors.

2. The network is dominated by recurrent inhibition.

3. The neurons receive large amount of stochastic background inputs.

The cortical micro circuit model consists of N neurons with N_E pyramidal neurons and N_I interneurons. The pyramidal neurons constitute of 80% of the total neuron population. The N_E neuron population is divided into stimuli sensitive population (fN_E) and non sensitive population ($(1-2f)N_E$). The participating neurons are connected in pyramid-pyramid, pyramid-interneuron, interneuron-interneuron, interneuron-pyramid neurons fashion. The neuron populations are described by the leaky integrate and fire neuron with the membrane potential $V(t)$ characterised as :-

$$C_m \frac{dV(t)}{dt} = -g_L(V(t) - V_L) - I_{syn}(t)$$

C_m is the membrane capacitance, g_L is membrane leak conductance, V_L is resting potential, $I_{syn}(t)$ is the total synaptic current. The $I_{syn}(t)$ has both AMPA and NMDA receptors. These external synaptic inputs send outside world stimuli and background noise to the architecture.

Reduced Model

The initial model by Wang[9] used $N_E = 1600$ and $N_I = 400$ leaky-and-integrate spiking neurons to simulate the model. Inorder to analytically study this model, Wong et. al. [10] reduced it to a two variable model. Inorder to achieve this reduction, the following steps were undertaken-

1. The first step in this reduction is to reduce the entire population of 2000 neurons to a population consisting of 4 units namely 2 discriminatory excitatory units, 1 non selective unit and 1 inhibitory unit. Wong used mean field approach to achieve this. In order to apply the mean field approach, proper estimation of the firing activity of the population and the synaptic input currents were made. First, the driving force of the synaptic input currents has been considered to be constant (Brunel [2]). Second, the contribution to the variance of the membrane potential is driven by external input to the population (the all-in-all connectivity within the neurons averages out the inter neuron contribution) as suggested by Renart et. al [6]. The σ is fixed at constant. Finally, the firing rate was expressed by the simplified input-and-output function (Abott and Chance [1]):-

$$r = \phi(I_{syn}) = \frac{C_{E,I} I_{syn} - I_{E,I}}{1 - exp[g_{E,I}(c_{E,I} I_{syn} - I_{E,I})]}$$

Here, ϕ is the function of the total synaptic input current

I_{syn} of a single cell. E,I represent either the excitatory or inhibitory neurons. $c_{E,I}$ is the gain factor and $g_{E,I}$ is the noise factor that determines the shape of the curvature of ϕ (which is linear threshold function for large g). This simplified model was derived from the first passage time formula of a single cell LIF model driven by a AMPA receptor mediated external gaussian noise.

Using this simplications and estimations, the entire neural population was able to be converted into 4 units (as mentioned initially). These units can be represented by 11 variables, mentioned below :-

$$\tau_r \frac{dr_i}{dt} = -r_i + \phi(I_{syn,i})$$

$$\tau_r \frac{dr_I}{dt} = -r_I + \phi(I_{syn,I})$$

$$\frac{S_{AMPA,i}}{dt} = -\frac{S_{AMPA,i}}{\tau_{AMPA}} + r_i$$

$$\frac{dS_{NMDA,i}}{dt} = -\frac{S_{NMDA,i}}{\tau_{NMDA}} + (1 - S_{NMDA,i})F(\psi(r_i))$$

$$\frac{dS_{GABA}}{dt} = -\frac{S_{GABA}}{\tau_{GABA}} + r_I$$

Here, $i = 1, 2, 3$ represent the 3 units namely 2 stimuli discriminatory excitatory neuron and 1 unit of non selective excitatory neuron. I is the inhibitory unit. $r_i(t)$ and r_I are the mean

firing rate of the excitatory and inhibitory units. S is the synaptic gating variable and τ is the decay time constant.

2. Using the mean field approach, the model is represented by 11 variables. This model can be further reduced into 8 variables by observing the activity of the non selective excitatory unit. As the firing rate of the non selective unit is more or less constant, it can be replaced by a constant mean rate of 2 Hz. However, this simplification does introduce certain consequences. The first being the difference between the previous model and the current model's firing rate is about 1 Hz. The second consequence is that we would neglect the slightly increased inhibition on the selective excitatory unit by the slightly elevated activity of the non selective unit.

Additionally, the inhibitory interneurons can be linearised as the instantaneous firing rate 8 Hz and the mean firing rate 8 to 15 Hz meakes the single cell input-output relation linear which can be expressed as :-

$$\phi(I_{syn}) = \frac{1}{g_2}(c_I I_I) + r_0$$

The self inhibitory coupling term lowers the effective firing rate by a factor of $1 + (c_I/g_2)J_{II}$. This removes the self consistancy calculation of the inhibitory population.

3. The final reduction of the neural model was achieved by

analysing the time membrane constant of the neurons and the gating variables. The membrane time constant of an instantenous cell can be ignored as the firing rate of a cell is instantenous [Brunel et. al. [3] and [4]]. Among the gating variables, S_{NMDA} has the longest time decay and hence dominates the time evolution of the system. The gating NMDA variable is defined as:-

$$\frac{dS_{NMDA,i}}{dt} = -\frac{S_{NMDA,i}}{\tau_{NMDA}}(1 - S_{NMDA,i})F(\psi_i)$$

Where, i represents the two excitatory stimuli discriminatory units and S_{NMDA} is the gating variable of NMDA receptor and τ_{NMDA} is the time membrane constant of that receptor.

The above estimations finally reduced the 2000 spiking neurons into a two variable model, defined as :-

$$\boxed{\begin{array}{l} \frac{dS_1}{dt} = G_1(S_1, S_2) = -\frac{S_1}{\tau_S} + (1 - S_1)\gamma H(x_1, x_2) \\ \frac{dS_2}{dt} = G_2(S_2, S_1) = -\frac{S_2}{\tau_S} + (1 - S_2)\gamma H(x_2, x_1) \end{array}}$$

Here, $H(x_1, x_2)$ and $H(x_2, x_1)$ are the firing rate of the two units. Again, x_1 and x_2 is defined as:-

$$\begin{array}{l} x_1 = J_{N,11}S_1 - J_{N,12}S_2 + I_0 + I_1 + I_{noise,1} \\ x_2 = J_{N,22}S_2 - J_{N,21}S_2 + I_0 + I_1 + I_{noise,2} \end{array}$$

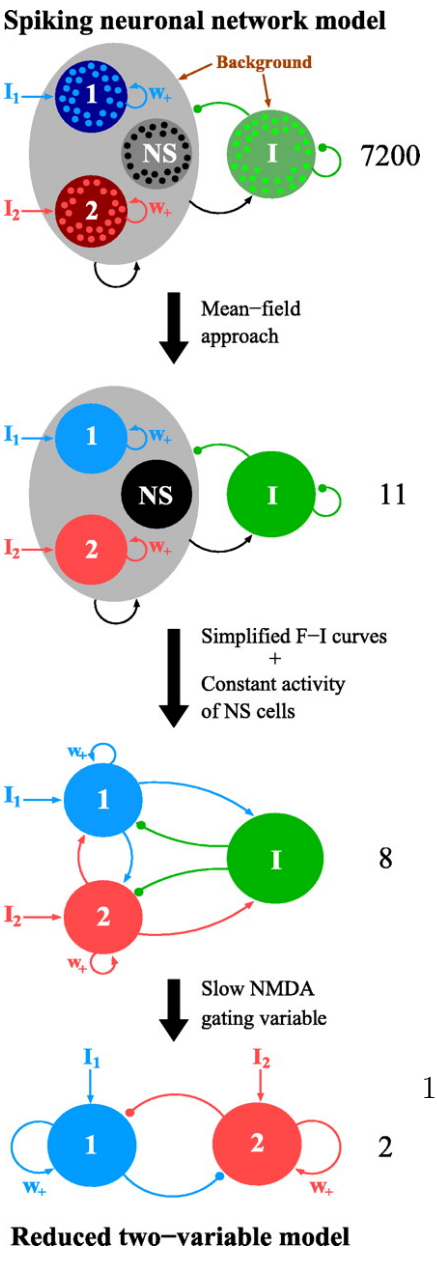

$I_{noise,i}$ is the noise term. I_0 is the common external input to both population. S is the gating variable. $J_{N,ij}$ are the effective coupling constants. $Fig2$ shows the entire reduction process.

Simulation and assignments

Package Requirement and Installation

We are using python 3.7 for simulating the network. The packages used are as follows:-

- Brian2
- neurodynex
- numpy
- matplotlib

As we are using Jupyter notebook, we installed the packages using conda.

To install a package, the command we use:-

```
pip install packageName
```

Installation of **Brian2** requires additional steps in anaconda. Listing them down here:-

- conda install -c conda-forge brian2
- conda config –add channels conda-forge

  Post this steps, normal installation and updation

- conda install brian2

For **pip** users, it is like normal package installation.

Findings and Analysis

In this chapter we would be discussing the various findings from the simulation and drawing a parallel with the mathematical/experimental observations. The analysis is divided into the following sections :-

Phase plane analysis

In order to get the phase plane of the network we determined the fixed points by setting $\frac{dS_1}{dt} = 0$ and $\frac{dS_2}{dt} = 0$. $Fig3$ shows the development of the phase plane starting from no external input to stimulus with increasing coherence.

In the absence of external stimulus the network has **five fixed points** out of which 3 are attractors and 2 are repellers. $Fig2.A$ shows the phase plane when no external stimulus is present.At this stage the network is unbiased and lies on the lower left attractor point (spontaneous stage). The other two attractors corresponds to those points where one of the neuron population shows self sustained behaviour.

$Fig2.B$ shows the phase plane when it has an unbiased external stimulus. Under such condition, the spontaneous stable

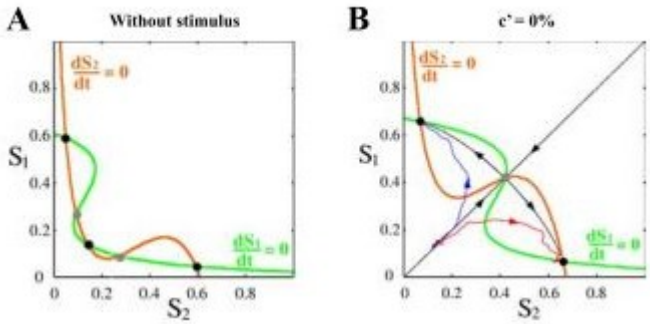

Figure 2: Phase Plane Analysis of Reduced Model with unbiased stimulus

point and the repellers collapses to form a saddle point. The two diagonals coming out of the saddle point each represent a stable and an unstable manifold. When the system starts in the stable manifold , it converges to the saddle point. This manifold divides the entire plane into two basins of attractors for each categorical choice. Whenever the system is at either of this basin, it gets attracted to that stable fixed point. Whenever, the system is in the unstable manifold, the system is repelled to either of the choices.

The model can also show delayed response version of the task. In this case, during the hold period, the choice is stored in either of the asymmetric stable nodes to be retrieved during decision making. A transient input post that can reset the model.

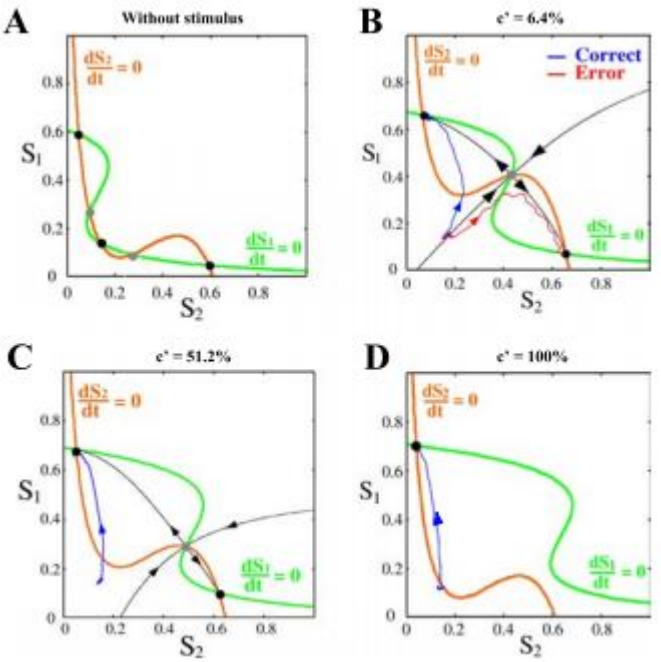

Figure 3: Phase Plane Analysis of Reduced Model

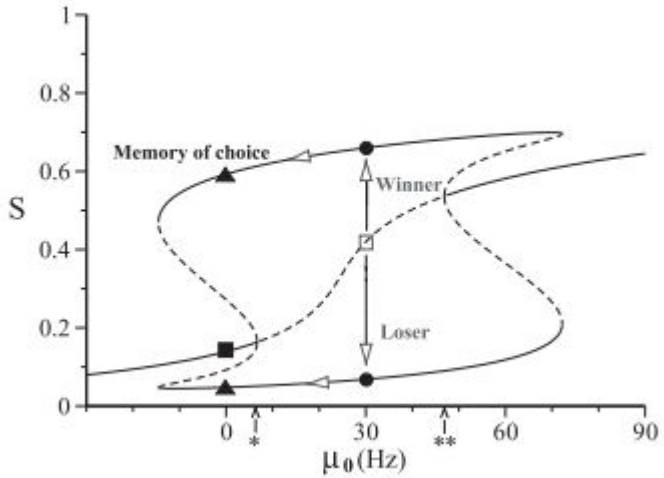

Figure 4: Bifurcation Diagram

This can be better visualised by a bifurcation diagram of selective population as function of stimulus strength μ_0 as shown in Fig 3.

At the onset of the experiment, the state is at a stable steady state (filled square). With the introduction of a stimulus, the system translates to a unstable state (empty square). In this state, the system goes to either of the stable branches (either winning or losing choice). Further, on removal of the stimuli due to hysteresis of the state , the system continues to state in that

state. Additionally at very high stimulus $\mu_0 > 47$ Hz, one of the steady state (the losing choice) annhilates leaving only one steady state choice to the system.

$Fig4$ shows the development of the phase plane in the presence of a biased stimuli with increasing $c\prime$ level. As can be seen with the increase in coherence, the attractor basin of the biased choice becomes larger and finally above a particular critical coherence value , the attractor basin of the other choice annhilates (Fig 3.D). Thus, above a particular $c\prime$, the model would always select the correct choice.

The biased external stimuli which favours one of the choices can also be used to explain another experimental observation. As already mentioned, with an increase in $c\prime$, the probability of choosing the favoured choice increases. This happens as the spontaneous state of the system gets located deeper and deeper into the favoured attractor basin (Fig 3.C). Thus noise and perturbations cannot dislocate the system into the stable manifold leading to extraction towards the saddle point or making an error choice. This location of spontaneous state deeper into the attractor basin of the favoured choice also explains decrease in decision time as the localtion of spontaneous stage makes it impervious to noise and leads to a quicker merging into attractor node.

Further, in case of trial error Fig 3.B (red line) in order for

the model to make a error choice, it will first travel along the stable manifold and would later diverge away from it into the error attractor. This diverging away takes time due to the ruins of the attractor [5] leading to a comparatively longer decision time in case of error trails than correct trials.

As has been mentioned above in case of low $c\prime$ value, the system initiates in/near the stable manifold and first converges towards the saddle ; further any perturbation pushes it into the unstable manifold leading to one of the categorical choices. Thus, we would next analyse the impact of the saddle node and the ruins of attractor on the integration time in case of low coherence and weak input μ_0. As the dynamics near the saddle is slow, the distance between S = (S_1, S_2) and S_{saddle} can be linearised and expressed as :-

$$\Delta S = a_1 v_1 exp(-t/\tau_{stable}) + a_2 v_2 exp(-t/\tau_{unstable})$$

Here, v_1 and v_2 are the eigenvectors of the saddle node (which is nothing but the stable and unstable manifolds). τ_{stable} and $\tau_{unstable}$ are the eigenvalues. a_1 and a_2 determined by the initial condition of the system, such that when the system initialises at the stable manifold the distance between the system and the saddle decreases in the order of $exp(-t/\tau_{stable})$ and if the system initialises in the unstable manifold , it distance between the system state and the saddle increases at a rate of $exp(-t/\tau_{unstable})$.

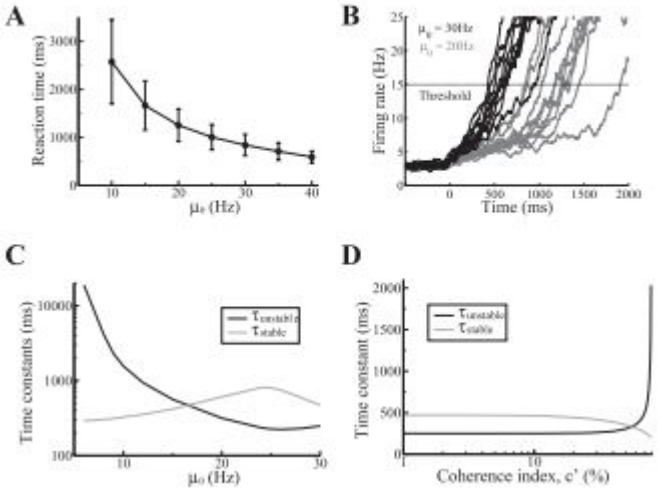

Figure 5: Slower dynamics due to Saddle

This linearization of the slow dynamics of the saddle area can successfully explain the longer decision time for weaker inputs μ_0.

Looking in Fig 5.*A* and 5.*C* shows that with a decrease in μ_0 the decision time increases , this increase can be paralleled with the increase in $\tau_{unstable}$ (which this model is able to show). However, this linearization tends to over emphasize the role of saddle on the system. First, it disregards the role of the stable manifold in the decision integration time , which cannot be ignored as the system's spontaneous stage lies on or near the stable

manifold. Additionally, noise and increase in $c\prime$ pushes the system away from the saddle region, further diminishing their role on the integration time.

The model also tried to explain through phase plane is the role of NMDA synapses on the model. Inorder the elicit the role of NMDA synapses on the excitatory units, we have to reintroduce AMPA synapses into the model. This was achieved by using the 11 variable model definition of the reduced model phase.

The final characteristic to be studied is the influence of Recurrent Strength w_+ on the model. Decreasing w_+ increases $\tau_{unstable}$ leading to the increase in decision time (as already discussed with respect to μ_0).

Also we were able to show that we the increase in w_+ , the reaction time decreases ; however the performance also drastically falls down. Likewise, the w_+ can be used to explain the diffusion model (system starts at stable manifold and then converges to one of the asymmetric attractor through unstable manifold). atleast qualitatively. However, as discussed previously, quantitatively this model does not adher to the diffusion model.

Analysing the phase plane of w_+ and μ_0 shows different regions of stability. Lower value of w_0 (Region I in fig 7.) shows the model incapable of making a decision as it would never reach the Competition phase of the plane. Similarly, for very high values of w_0, the competition of the model cannot be replicated . This

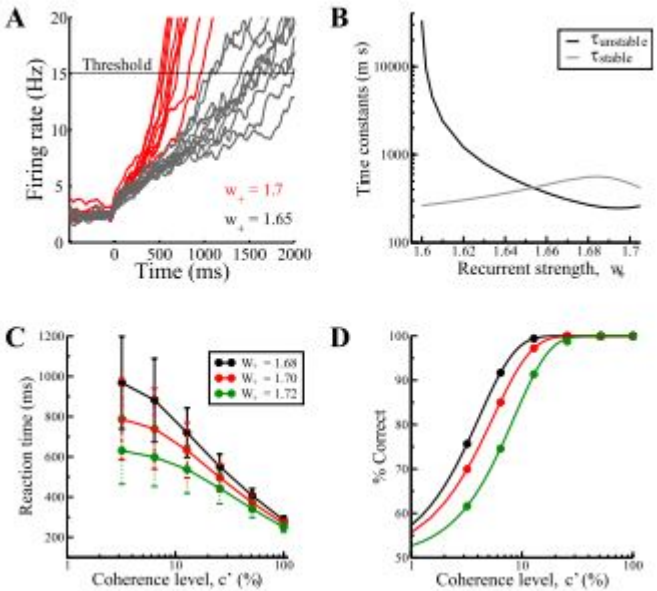

Figure 6: Recurrent Strength Analysis

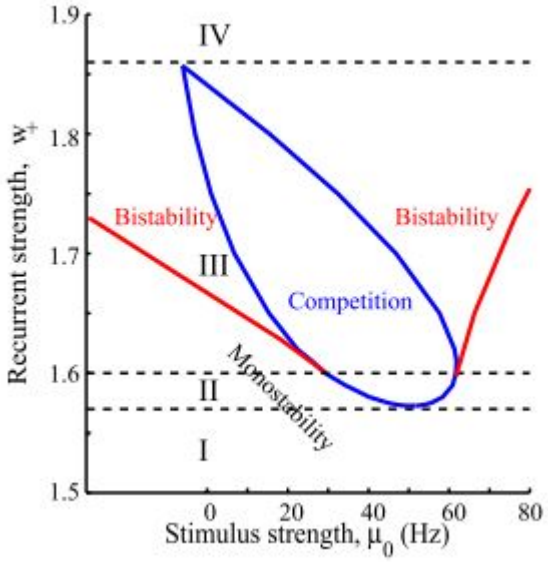

Figure 7: Recurrent Strength Analysis

portion shows the annhilation of the losing aymmetric attractor. For a small portion of w_0, the competition dynamics of the model can be replicated.

Simulation Findings

13.1.1.Understanding Brian2 Monitors

For each of the four subpopulations, find the variable name of the corresponding NeuronGroup.

The four subpopulations are **inhib_pop** which is the inhibitory population, **excit_pop_A**, **excit_pop_B** and **excit_pop_Z** which are the excitatory population.

Each NeuronGroup is monitored with a PopulationRateMonitor, a SpikeMonitor, and a StateMonitor. Find the variable names for those monitors. Have a look at the Brian2 documentation if you are not familiar with the concept of monitors.

For the inhibitory population, the PopulationRateMonitor, SpikeMonitor and StateMonitor is **rate_monitor_inhib,spike_monitor_inhib voltage_monitor_inhib**.
For the excitatory populations, the PopulationRateMonitor, SpikeMonitor and StateMonitor are **rate_monitor_A, spike_monitor_A, voltage_monitor_A** , **rate_monitor_B, spike_monitor_B, voltage_monitor_B** and **rate_monitor_Z, spike_monitor_Z, voltage_monitor_Z**.

Which state variable of the neurons is recorded by the StateMonitor?

The voltage "v" is being recorded.

13.2 Stimulating the decision making circuit

express the difference μ_{left} - μ_{right} in terms of μ_0 and c

The difference is $\mu_0 * c$.

Find the distribution of the difference $v_{left} - v_{right}$.

$v_{left} \approx \mathrm{N}(\mu_{left}, \sigma^2)$
$v_{right} \approx \mathrm{N}(\mu_{right}, \sigma^2)$

v_{left} - $v_{right} \approx v_{left}$ + (-1) v_{right}
$\approx \mathrm{N}(\mu_{left} - \mu_{right}, 0)$

Find the default values of of μ_0 and σ^2

μ_0 is 160 Hz and σ^2 = is 20 Hz.
What are the mean firing rates for c =-0.2

Bibliography

[1] LF Abbott and Frances S Chance. Drivers and modulators from push-pull and balanced synaptic input. *Progress in brain research*, 149:147–155, 2005.

[2] Nicolas Brunel. Dynamics of sparsely connected networks of excitatory and inhibitory spiking neurons. *Journal of computational neuroscience*, 8(3):183–208, 2000.

[3] Nicolas Brunel and Xiao-Jing Wang. Effects of neuromodulation in a cortical network model of object working memory dominated by recurrent inhibition. *Journal of computational neuroscience*, 11(1):63–85, 2001.

[4] Nicolas Fourcaud and Nicolas Brunel. Dynamics of the firing probability of noisy integrate-and-fire neurons. *Neural computation*, 14(9):2057–2110, 2002.

[5] John H Hubbard and Beverly H West. *Differential equations: a dynamical systems approach: higher-dimensional systems*, volume 18. Springer Science & Business Media, 2012.

[6] Alfonso Renart, Nicolas Brunel, and Xiao-Jing Wang. Mean-field theory of recurrent cortical networks: working memory circuits with irregularly spiking neurons. *Computational*

neuroscience: A comprehensive approach, pages 432–490, 2003.

[7] Jamie D Roitman and Michael N Shadlen. Response of neurons in the lateral intraparietal area during a combined visual discrimination reaction time task. *Journal of neuroscience*, 22(21):9475–9489, 2002.

[8] Michael N Shadlen and William T Newsome. Neural basis of a perceptual decision in the parietal cortex (area lip) of the rhesus monkey. *Journal of neurophysiology*, 86(4):1916–1936, 2001.

[9] Xiao-Jing Wang. Probabilistic decision making by slow reverberation in cortical circuits. *Neuron*, 36(5):955–968, 2002.

[10] Kong-Fatt Wong and Xiao-Jing Wang. A recurrent network mechanism of time integration in perceptual decisions. *Journal of Neuroscience*, 26(4):1314–1328, 2006.